HHS Public Access

Author manuscript

Biochem Pharmacol. Author manuscript; available in PMC 2019 September 01.

Published in final edited form as:

Biochem Pharmacol. 2018 September ; 155: 82–91. doi:10.1016/j.bcp.2018.06.024.

INTERACTIONS OF ENDOCANNABINOID VIRODHAMINE AND RELATED ANALOGS WITH HUMAN MONOAMINE OXIDASE-A AND -B

Pankaj Pandey[#1], **Narayan D. Chaurasiya**[#2], **Babu L. Tekwani**[1,2,‡,*], and **Robert J. Doerksen**[1,2,*]

[1]Department of BioMolecular Sciences, National Center for Natural Products Research, Research Institute of Pharmaceutical Sciences, School of Pharmacy, University of Mississippi, University MS 38677

[2]National Center for Natural Products Research, Research Institute of Pharmaceutical Sciences, School of Pharmacy, University of Mississippi, University MS 38677

[‡] Division of Drug Discovery, Southern Research, Birmingham, AL 35205

[#] These authors contributed equally to this work.

Abstract

The endocannabinoid system plays an important role in the pathophysiology of various neurological disorders, such as anxiety, depression, neurodegenerative diseases, and schizophrenia; however, little information is available on the coupling of the endocannabinoid system with the monoaminergic systems in the brain. In the present study, we tested four endocannabinoids and two anandamide analogs for inhibition of recombinant human MAO-A and -B (monoamine oxidase). Virodhamine inhibited both MAO-A and -B (IC_{50} values of 38.70 and 0.71 μM, respectively) with ~55-fold greater inhibition of MAO-B. Two other endocannabinoids (noladin ether and anandamide) also showed good inhibition of MAO-B with IC_{50} values of 18.18 and 39.98 μM, respectively. Virodhamine was further evaluated for kinetic characteristics and mechanism of inhibition of human MAO-B. Virodhamine inhibited MAO-B (K_i value of 0.258 ± 0.037 μM) through a mixed mechanism/irreversible binding and showed a time-dependent irreversible mechanism. Treatment of Neuroscreen-1 (NS-1) cells with virodhamine produced significant inhibition of MAO activity. This observation confirms potential uptake of virodhamine by neuronal cells. A molecular modeling study of virodhamine with MAO-B and its cofactor flavin adenine dinucleotide (FAD) predicted virodhamine's terminal $-NH_2$ group to be positioned near the N5 position of FAD, but for docking to MAO-A, virodhamine-s terminal $-NH_2$ group was far away (~6.52 Å) from the N5 position of FAD, and encountered bad contacts with nearby water molecules. This difference could explain virodhamine's higher potency and preference for MAO-

[*]Corresponding authors: Robert J. Doerksen, rid@olemiss.edu, Phone: 1-662-915-7052; Fax: 1-662-915-6557; Babu L. Tekwani, btekwani@southernresearch.org, Phone 1-205-581-2205; Fax: 1-662-915-7062.

Declarations of interest: none

B. The binding free energies for the computationally-predicted poses also showed that virodhamine was selective for MAO-B. These findings suggest potential therapeutic applications of virodhamine for the treatment of neurological disorders.

Keywords

MAO-B; endocannabinoids; docking; enzyme kinetics; virodhamine

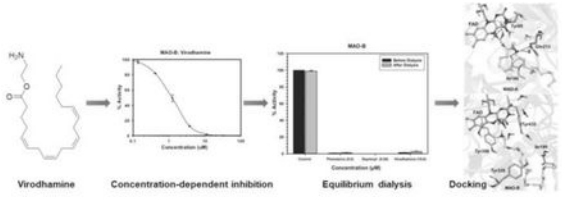

1. Introduction

Monoamine oxidase (MAO), a flavin adenine dinucleotide (FAD)-dependent mitochondrial enzyme located on the outer mitochondrial membrane, catalyzes oxidative deamination of a variety of endogenous amines including dopamine, norepinephrine (noradrenaline), epinephrine (adrenaline), serotonin, phenylethylamine, and xenobiotic amines such as benzylamine and kynuramine [1, 2]. MAO exists in two immunologically and catalytically distinct isoforms, type A (MAO-A) and type B (MAO-B), having their own different distribution in human tissue, substrate preference, and inhibitor specificity [3]. The amino acid sequences deduced from cDNA clones that encode MAO-A and -B show a 70% homology [3]. This high homology makes identifying selective and clinically useful inhibitors for either of the MAO subtypes challenging. MAOs play important roles in brain function and development, and therefore MAO inhibitors have a wide range of potential therapeutic uses [4, 5]. Non-selective MAO inhibitors and selective MAO-A inhibitors have shown potential for treating depression, panic disorder, and other anxiety disorders when first-line treatments show poor results [6, 7]. Selective inhibitors of MAO-B, by contrast, have shown high potential in treating Parkinson's disease [8, 9] and Alzheimer's disease [7, 10].

The endocannabinoids are highly lipophilic molecules that are naturally produced or made on demand during physiological and/or pathological events by the human body and released in response to activation of metabotropic glutamate receptors or postsynaptic depolarization to stimulate cannabinoid receptors [11-14]. The endocannabinoid system includes two receptor subtypes, cannabinoid receptors 1 (CB1) and 2 (CB2), their endogenous ligands (endocannabinoids) and endocannabinoid-degrading enzymes such as fatty acid amide hydrolase (FAAH) and monoacylglycerol lipase (MAGL). Endocannabinoids are widely distributed throughout the body: in the brain, organs, connective tissues, immune system and glands. Anandamide (AEA), 2-arachidonoylglycerol (2-AG), and several other endogenous cannabinoids such as noladin ether (CB1/CB2 agonist), virodhamine (CB1 partial/antagonist and CB2 agonist) and N-arachidonyl-dopamine (CB1 agonist) are lipid mediators and have the C20:4 (20 carbons and 4 double bonds) moiety in their structure [14].

There is no exact mechanism or detailed information available that describes the effect of cannabinoids on monoaminergic neurotransmission, and the link between the endocannabinoid system and the MAO system remains unclear. Little is known about the regulation of dopamine, norepinephrine, or serotonin catabolism in cannabinoid addiction [15] or the role of cannabinoids/endocannabinoids on MAO functions [16]. Several studies have shown that the endocannabinoid system impacts mood regulation/anxiety [17], depression, and other neuropsychiatric disorders [12], which are associated with an imbalance in glutamatergic, GABAergic, glycinergic, cholinergic, serotonergic and noradrenergic neurotransmissions [18, 19]. Bambico *et al.* [20] showed that cannabinoid drugs might potentiate monoaminergic neurotransmission and hippocampal neurogenesis via distinct pathways compared to classical antidepressants, which may provide an alternative drug class for treating mood and other neuropsychiatric disorders. Similarly, Ahanasiou *et al.* [21] reported that endocannabinoids, phytocannabinoids, and synthetic cannabinoid receptor agonists directly alter integrated mitochondrial function when cannabinoid receptors were knocked down. An *in vivo* study by Hill *et al.* [22] revealed that the chronic administration of a non-selective irreversible MAO inhibitor, tranylcypromine, altered the endocannabinoid system through reduced anandamide content and increased CB1 receptor density in the hippocampus and prefrontal cortex, but did not show any direct CB1 receptor binding. Similarly, the endocannabinoid system is down-regulated in the hippocampus by chronic stress or glucocorticoid administration [23]. These data suggest that monoaminergic neurotransmission could be involved in the regulation of the endocannabinoid system and may play a potential role in mood disorders. Fisar's study [16] indicates that endocannabinoids can modulate monoaminergic neurotransmission in the brain by their direct effect on MAO function, in addition to CB1 receptor activation. Fisar [16] tested three cannabinoid receptor agonists, anandamide, tetrahydrocannabinol (Δ^9-THC), and WIN55212-2, for MAO activity in a crude mitochondrial fraction isolated from pig brain cortex and found MAO inhibition only at high concentrations. However, earlier studies found contrary effects of THC on MAO activity: THC elicited inhibitory [24], stimulatory [25], or no pharmacological effects [26], according to the different references.

Virodhamine is a partial agonist/antagonist at the CB1 receptor and acts as a full agonist at the CB2 receptor. *In vitro* data revealed that virodhamine can act as an endogenous antagonist at the CB1 receptor in the presence of anandamide [27]. Virodhamine also exhibits vasorelaxant activities in isolated small mesenteric artery from rat [28]. Porter et al. [27] found significant levels of virodhamine in human hippocampus and in various tissues in rat and the levels were similar to those of anandamide. In other rat tissue, the levels of virodhamine were significantly higher than those of anandamide. The level in human hippocampus was 5.3 picomoles/g and in rat hippocampus was 16.3 picomoles/g. This level is high enough to lead to significant effects such as reported by Porter et al. [27]

With the above-mentioned points in mind, the present study investigated *in vitro* effects of four endocannabinoids and two anandamide analogs (Fig. 1) against human MAO-A and -B activities to determine the role of the cannabinoids in regulation of neurotransmitter monoamines. To the best of our knowledge, we report the first *in vitro* effects of endocannabinoids and related analogs against human MAO-A and -B activities. The study was further extended to evaluation of binding and interaction of virodhamine with human

MAO-B, considering enzyme-kinetics, enzyme–inhibitor complex formation with equilibrium dialysis dissociation, and computational docking analysis of virodhamine to X-ray crystal structures of MAO-A and -B.

2. Materials and Methods

2.1 Reagents and chemicals

The recombinant human monoamine oxidases (hrMAO-A and -B) were procured from BD Biosciences (Bedford, MA, USA). Kynuramine dihydrobromide, 4-hydroxyquinoline, clorgyline, *R*-(−)-deprenyl hydrochloride, phenelzine sulfate, potassium phosphate and dimethyl sulfoxide (DMSO) were obtained from Sigma Chemical Co. (St. Louis, MO, USA). Virodhamine and related analogs were obtained from Tocris Bioscience (Bristol, UK). Safinamide was obtained from TCI Chemicals, USA. The Falcon flat-bottom 384-well white microplates, used for the MAO assays, were procured from Fisher Scientific Co., USA.

2.2 Determination of inhibition effect (IC_{50}) against MAO-A and -B

The *in vitro* assays were performed to measure the inhibition effects of virodhamine and related analogs on enzymatic activities of recombinant human MAO-A and -B. Phenelzine (a nonselective MAO inhibitor), deprenyl (a selective MAO-B inhibitor), and clorgyline (a selective MAO-A inhibitor) were tested simultaneously as reference standards [29]. Stock solutions (10 mM) of the compounds were prepared in DMSO. The compounds were serially diluted in enzyme assay buffer [30]. The assay tolerates the highest DMSO concentration of 0.1% without any effect of the solvent on the enzyme activities. The MAO-A and -B activities were determined by fluorometric kynuramine deamination assays [30, 31]. The assays were performed in white flat-bottom 384-well microplates. The MAO-A and -B inhibition activities (IC_{50} values) of virodhamine and related analogs were determined using a fixed concentration of the substrate (80 μM for MAO-A and 50 μM for MAO-B) and varying concentrations of test compounds (0.01 to 100 μM). These substrate concentrations, which are based on Km values of the recombinant human MAO-A and -B for kynuramine [31], were used as recommended by BD Biosciences. The inhibition constants (IC_{50} values) were computed by analysis of dose-response inhibition curves with the MS Excel-based XLFit plug-in program.

2.3 Enzyme kinetics and mechanism studies

Assays were performed at varying concentrations of kynuramine (1.90 to 500 μM) and at particular fixed concentrations of the test inhibitor for determination of the enzyme inhibition constants (Ki) for inhibition of MAO-A and -B with virodhamine. In addition to the controls without inhibitor, two concentrations (one below and one above the IC_{50} values) of the inhibitor were tested to determine the K_M and V_{max} values in the presence of inhibitor. The results are presented as double reciprocal Lineweaver–Burk plots and the kinetic data, namely K_M, V_{max} and Ki values, were calculated in the Enzyme-Kinetics module of SigmaPlot 12.3 using the Michaelis-Menten equation. The data on enzyme activity at different concentrations of the substrate and at at least two fixed concentrations of the test inhibitor were entered into a SigmaPlot data sheet for the curve fitting and graphic

analysis of the enzyme kinetics data. The results were analyzed for the type of inhibition. The Ki values for mixed-type enzyme inhibition, as observed in the case of virodhamine, are computed by the Enzyme-Kinetics module as the mean of Ki values, i.e., Kic for the competitive and Kiu for the uncompetitive parts of inhibition.

2.4 Effect of Virodhamine on MAO activity in Neuroscreen-1 (NS-1) cells

The Neuroscreen-1 (NS-1) cells (a subclone of rat pheochromocytoma neuroendocrine PC12 cells) were cultured as described in our previous publication [32]. The NS-1 cells in a suspension culture were treated with virodhamine (100 μM) or deprenyl (1.0 μM) for 12 hours. The cell lysates were prepared and MAO activity was determined in control and treated cell lysates as described in section 2.2.

2.5 Analysis of binding characteristics of virodhamine with MAO-B

The characteristics of virodhamine binding for inhibition of MAO-B were examined by incubating the recombinant enzyme protein with high concentrations of the inhibitor followed by an extensive equilibrium dialysis of the enzyme-inhibitor complex and the recovery of catalytic activity of the protein. Recombinant human MAO-B (50 μg/mL protein) was incubated with virodhamine (10.0 μM) in an enzyme incubation mixture of 1 mL containing 100 mM potassium phosphate buffer (pH 7.4). After incubation for 20 minutes at 37 °C, the reaction was terminated by chilling the reaction mixture on ice. The samples with the enzyme-inhibitor complex were dialyzed against potassium phosphate buffer for 14-16 hours at 4 °C (changing buffer three times). A similar process was run for the enzyme control (without inhibitor) and the enzyme catalytic activity was measured before and after dialysis. After dialysis of the enzyme-inhibitor incubation mixture, retrieval of the enzyme activity delivered important information concerning the irreversibility of the virodhamine binding with the enzyme.

2.6 Time-dependent enzyme inhibition assay with MAO-B

In order to analyze the time-dependent inhibition of the catalytic function of MAO-B by virodhamine, the enzyme was pre-incubated for different time intervals (0-15 min) with virodhamine at a concentration (2.5 μM) that produced >60% inhibition of the enzyme activity. Deprenyl (0.100 μM) was tested as a control MAO-B inhibitor. Controls in the absence of inhibitors were also run simultaneously. The results were analyzed with the percent enzyme activity remaining plotted against the pre-incubation time to evaluate the time-dependent enzyme inhibition.

2.7 Computational analysis of interactions of virodhamine with human MAO-A and -B

The X-ray crystal structures of human MAO-A (PDB ID: 2Z5X) [33] and MAO-B (PDB ID: 1OJ9) [34] were downloaded from the Protein Data Bank (https://www.rcsb.org/) and prepared for proper ionization state, bond order and missing side chains using Maestro [35]. Conserved water molecules were retained for docking study. In order to identify conserved waters in the crystal structures of MAO-A and -B, an alignment and overlay of water molecules near the ligand binding site was used, based on 2Z5Y [33] and 2Z5X [33] X-ray crystal structures for MAO-A, and on 2XCG [36], 1OJ9 [34], 1S2Q [37], 4A79 [38], 2V5Z

[39], 2BYB [40], and 2VRM [41] crystal structures for MAO-B. Virodhamine and kynuramine were sketched in Maestro, and prepared and energy minimized at physiological pH of 7.4 using the LigPrep [42] module of the Schrödinger software. The active sites of the MAO-A and -B proteins were each defined by the centroid of the co-crystallized ligand present in 2Z5X and 1OJ9, respectively. For comparison, we also performed docking considering N5 of FAD as the centroid of the active site. Virodhamine and kynuramine were docked using the InducedFit [43] docking protocol by applying the extra-precision (XP) [44] docking method and the top 10 poses were kept for analysis. Binding free-energy calculations were further performed for the best docking poses using the Prime MM-GBSA module [45] implemented in the Schrödinger software.

3. Results

3.1 Determination of inhibitory effects of virodhamine and related analogs on MAO-A and -B

This study investigated the effects of virodhamine and related analogs (Fig. 1) on the *in vitro* activity of monoamine oxidase (MAO), the enzyme responsible for metabolism of monoamine neurotransmitters and affecting brain development and function. The effects of endocannabinoids and related analogs on recombinant human MAO-A and -B activity were assessed in comparison with deprenyl, a well-known potent irreversible selective MAO-B inhibitor, phenelzine, a potent nonselective MAO-A and -B inhibitor, and safinamide, a selective MAO-B inhibitor. Among the tested cannabinoids, virodhamine was the most potent inhibitor of MAO-B. Virodhamine inhibited both MAO-A and -B (IC_{50} values of 38.70 μM and 0.71 μM, respectively), with ~55-fold greater inhibition of MAO-B (Table 1, Fig. 2). Two other endocannabinoids, noladin ether and anandamide, also showed greater inhibition of MAO-B than of MAO-A, with MAO-B IC_{50} values of 18.18 μM and 39.98 μM, respectively (Table 1); however, the inhibition of MAO-B by these two endocannabinoids was significantly lower compared to virodhamine (Table 1).

3.2 Evaluation of MAO-B inhibition kinetic of virodhamine

Virodhamine was further evaluated for kinetic characteristics and the mechanism of inhibition of the human MAO-B, since it was the most active at MAO-B. Virodhamine was tested for MAO-B inhibition at varying concentrations of kynuramine, a nonselective substrate, to investigate the nature of inhibition of the enzyme. Two additional concentrations of the inhibitor (one below and another above the IC_{50} value) were selected. The enzyme kinetics data are presented as double reciprocal Lineweaver–Burk plots (Fig. 3). The Ki (inhibition constant) values and other enzyme kinetic parameters were computed with the SigmaPlot 12.3 enzyme module. Virodhamine inhibited the catalytic functions of MAO-B (Ki value of 0.258 ± 0.037 μM) through a mixed enzyme inhibition mechanism, as demonstrated by Table 2 and Figs. 3 and 4.

3.3 Analysis of binding of virodhamine with MAO-B

The characteristics of binding of virodhamine with recombinant human MAO-B was investigated through enzyme-inhibitor complex dissociation by equilibrium dialysis. Virodhamine was incubated with the recombinant enzyme (MAO-B) protein for 20 minutes.

The resulting enzyme-inhibitor complex mixture was dialyzed overnight. The catalytic activity of the enzyme was determined before and after the dialysis. The control reaction, which was done on the recombinant human MAO-B protein incubated without the inhibitor, lost about 5% of the enzyme activity during overnight dialysis. Incubation of MAO-B with virodhamine (10.0 μM) caused almost complete inhibition of catalytic activity of the enzyme. After overnight dialysis, only 2.644 ± 0.450% of the activity of the enzyme was recovered from the enzyme-virodhamine incubation mixture. Similar treatment of the enzyme with phenelzine (a non-selective MAO-A/B inhibitor) and deprenyl (a selective MAO-B inhibitor) also showed irreversible inhibition/binding with the human MAO-B protein. This indicated formation of un-dissociable enzyme-inhibitor complexes. Thus, the binding of virodhamine with MAO-B was found to be irreversible (Fig. 4).

3.4 Time-dependent inhibition of MAO-B with virodhamine

The time-dependent binding inhibition of MAO-B by virodhamine was studied as described in the Material and method section. Pre-incubation with 0.25 μM virodhamine for 0-15 min produced ~55-70% inhibition (Fig. 5). The results showed that inhibition of MAO-B by virodhamine was time-dependent, similar to that by deprenyl.

3.5 Effect of treatment of Neuroscreen-1 (NS-1) neuroendocrine cells with virodhamine on MAO activity

The Neuroscreen-1 (NS-1) cells (a subclone of rat pheochromocytoma neuroendocrine PC12 cells) were treated with virodhamine, ethanol or deprenyl for 12 hours. The MAO activity was determined in the cell lysates prepared from control (untreated) and treated cells (Fig. 6). Treatment with deprenyl resulted in >90% inhibition in MAO activity, while treatment with virodhamine caused >60% inhibition of MAO activity.

3.6 Molecular modeling study

Docking of virodhamine to MAO-A or MAO-B was done considering the co-crystallized ligand as the centroid of docking. However, for kynuramine, which is a considerably smaller molecule than virodhamine or the co-crystalized ligands, docking using the centroid of the co-crystallized ligand gave variable poses (different docking poses for which it looked unlikely that kynuramine could act as a substrate), with kynuramine rather far from N5 (>4 Å), whereas using N5 as the centroid of docking gave a pose with kynuramine's terminal amine close to N5 (< 2 Å). So, we used the latter approach for kynuramine. The docking protocol was validated by self-docking in which the X-ray structure native ligands, harmine and 1,4-diphenyl-2-butene, were docked into their corresponding proteins stuctures, of MAO-A and -B, respectively. We calculated the RMSD between the docked and experimental poses to be 0.34 Å and 0.53 Å, respectively (Fig. 7), verifying that the docking protocol worked well.

The molecular docking study in the presence of conserved waters showed that virodhamine binds preferentially to MAO-B (Fig. 8) (Glide docking score = −11.26 kcal/mol, Emodel score = −57.79 kcal/mol, and MM-GBSA free-energy ΔG = −48.0 kcal/mol) compared to MAO-A (Fig. 8) (Glide score = −10.17 kcal/mol, Emodel score = −85.92 kcal/mol, and ΔG = −33.96 kcal/mol) (Table 3). When all the conserved waters were removed from MAO-A

and -B, the docking scores were considerably poorer for MAO-A and -B [GlideScore (MAO-B) = −9.96 kcal/mol, GlideScore (MAO-A) = −6.51 kcal/mol). These observations suggest the role of conserved waters in the ligand interactions with MAO-A and -B.

Docking of virodhamine to MAO-B (PDB ID: 1OJ9) showed that the terminal -NH_2 group of virodhamine faced towards N5 of FAD with an N-N distance of 3.12 Å. However, docking of virodhamine to MAO-A (PDB ID: 2Z5X) showed that its terminal -NH_2 group was far away (6.52 Å) from N5 of FAD, and virodhamine also encountered bad contacts with nearby water molecules. This difference could explain virodhamine's higher potency and binding preference for MAO-B over MAO-A. Binding free energies for the computationally-predicted poses of virodhamine (MAO-A = −33.97 kcal/mol and MAO-B = −48.00 kcal/mol) also agree with the experimental IC_{50} results, that virodhamine binds better to MAO-B. Virodhamine's terminal -NH_2 group (which should be protonated at physiological pH) exhibited cation-π interactions with Tyr398 and was surrounded by hydrophobic residues of MAO-B: Tyr60, Cys172, Ile198, Phe343, and Tyr435 were all within 4 Å. The terminal -NH_2 group of virodhamine in MAO-A formed hydrogen bonds with Ile180 (backbone) and Gln215 (side chain) (Fig. 8). In MAO-B, the terminal alkyl group of virodhamine extended beyond the gate-keeper residues (Ile199 and Tyr326) and the extended alkyl chain exhibited strong hydrophobic interactions with these residues. In contrast, the docking of kynuramine (a non-selective MAO substrate) resulted in a poorer docking score (GlideScore = −7.67 kcal/mol) and binding free-energy (ΔG = −36.71 kcal/mol) compared to virodhamine, even though the terminal -NH_2 of kynuramine and terminal -NH_2 of virodhamine aligned almost identically (Fig. 9 and Table 3). These modeling data show that virodhamine exhibited strong non-covalent binding interactions with MAO-B.

4. Discussion

Our *in vitro* findings demonstrate MAO-B inhibitory pharmacological function of the endocannabinoid virodhamine. An earlier study has also investigated the effects on MAO-A and -B of cannabinoids and the endocannabinoid anandamide [16, 25]. The study conducted by Fisar et al. [16] employed crude mitochondrial enzyme preparations isolated from pig brain cortex as the source for MAO for the assays. Serotonin and phenylethylamine were employed as MAO-A and –B selective substrates, respectively, for inhibition by the phytocannabinoid Δ^9-tetrahydrocannabinol (THC), the endocannabinoid anandamide and a synthetic cannabinoid receptor agonist WIN 55,212-2 (WIN). Fisar et al. reported much weaker IC50 values of 750 μM and 1668 μM for inhibition of MAO-A and –B, respectively, by anandamide. Our work is the first report of inhibition of pure recombinant human MAO-A and -B with virodhamine and related analogs. Virodhamine displayed promising MAO-B inhibitory activity with IC_{50} values in the submicromolar range, and with >54-fold preference towards MAO-B compared to MAO-A (Fig. 2). Two other endocannabinoids (noladin ether and anandamide) also showed greater inhibition of MAO-B than MAO-A (Table 1). Similarly, an anandamide analog, (*R*)-(+)-methanandamide also exhibited MAO-B inhibitory activity with IC_{50} value in the micromolar range. Interestingly, five of the six compounds tested preferentially inhibited MAO-B and were inactive (up to 100 μM, the highest concentration tested) against MAO-A. For the exception, oleylethanolamide, its

higher degree of saturation in the alkyl moiety (only one isolated double bond) led to no activity of oleylethanolamide against either isoform of MAO.

In the present study, all the tested compounds shared the common arachidonoyl tail structure but differed in their hydrophilic head groups (Fig. 1). The critical micellar concentrations (CMC) reported by Glick *et al.* [46] for arachidonic acid and arachidonoyl alcohol were 73 μM and 30 μM, respectively, while Pearlman *et al.* [47] mentioned that the CMC value for arachidonic acid was ~30 μM. Moreover, Baur *et al.* [48] reported the CMC value for 2-AG and the related structure NA-glycine to be 4.2 ± 0.5 μM and >100 μM, respectively. The concentration of virodhamine required to inhibit MAO-B (IC_{50} = 0.7 μM) is well below the reported CMC values for the virodhamine analogs. Other analogs such as 2-AG, noladin ether, anandamide, and *R*-methanandamide did not show any solubility issues. Additionally, no flat curves were found for the dose-response inhibition of MAO-B by virodhamine or analogs. These points rule out any impact of the formation of micelles by these compounds on their levels of enzyme inhibition at the concentrations tested.

To characterize the kinetics and the mechanism of inhibition mode of the endocannabinoid virodhamine, we incubated it with MAO-B at two concentrations, one below and another above its IC_{50} value. Virodhamine was tested for MAO-B inhibition kinetics at varying concentrations of substrate kynuramine. The enzyme kinetics Lineweaver–Burk plots confirmed that virodhamine inhibited MAO-B (Ki value of 0.258 ± 0.037 μM) through mixed mechanism/irreversible binding (Table 2 and Fig. 3). We also performed a dialysis study to characterize the inhibition mode of virodhamine by incubating it with MAO-B at a concentration equal to 5 times its IC_{50} and subsequently dialyzed it overnight against buffer solutions. The positive control, R-(−)-deprenyl, an irreversible MAO-B inhibitor, was similarly incubated and dialyzed overnight against buffer solutions. As a negative control, MAO-B was dialyzed in the absence of virodhamine. The results of the dialysis study showed that virodhamine is an irreversible MAO-B inhibitor because dialysis did not restore the enzyme activity observed with the positive control (Fig. 4). The enzyme-inhibition kinetics and ligand interactions analysis with equilibrium dialysis suggested irreversible binding of virodhamine with human MAO-B. In addition, the time-dependent binding inhibition assay of MAO-B with virodhamine showed that inhibition of MAO-B by virodhamine was time-dependent. Selegiline and rasagiline, well-known irreversible inhibitors of MAO-B, are used clinically for the treatment of Parkinson's disease [49]. Safinamide is a reversible MAO-B inhibitor which has recently been approved for Parkinson’s disease treatment [9]. Our results suggest potential therapeutic application of virodhamine for the treatment of Parkinson’s disease. Selective irreversible inhibitors of MAO-B have also shown promise for treatment of depression and Attention Deficit Hyperactivity Disorder (ADHD) [49, 50]. Selective MAO-B inhibition also leads to increase in endogenous β-phenylethylamine (PEA) levels in the brain [51]. The increase in endogenous PEA levels produces dopamine release-promoting activity and contributes to positive effects on motor features and behavior [52].

The computational docking studies provided further insights into selective interactions of virodhamine with the human MAO-B. Virodhamine binds in an extended conformation and fits reasonably well into the binding cavities of both MAO-A and MAO-B. However,

virodhamine binds tightly to MAO-B by forming π-π stacking and strong hydrophobic interactions with nearby amino acid residues (Fig. 8). This allows strong van der Waals contacts with active site residues in both cavities, which leads to potent inhibition of the enzyme function. The docking poses showed the terminal alkyl moiety of virodhamine situated within the entrance cavity and the amino groups (-NH_2) orientated towards the FAD cofactor in the substrate-binding cavity. Additionally, the conserved water molecules within the enzyme active site were important for interaction of virodhamine with MAO-B. The overall characteristics of the interactions of virodhamine with human MAO-B are similar to those of kynuramine (Fig. 9), the non-selective MAO-A/B substrate employed in these studies, and also to those reported recently for dopamine, the selective MAO-B substrate [53].

The importance of the endocannabinoid system in mood disorder and depression is generally potentiated through monoaminergic neurotransmission and hippocampal neurogenesis [20], which opens the possibility for researchers to look for CB ligands as new drugs for mood or psychotropic disorders. There are functional neural interactions between the dopamine receptor systems and the cannabinoid receptor systems [54]. The interactions between these two receptor systems may be important in addiction, Parkinson's disease, and schizophrenia. The selective MAO-B inhibitory property of virodhamine and other related analogs reported in this study suggests the potential of these analogs to modulate the levels of biogenic monoamines in brain and peripheral tissues. The results reported present the scope for additional neuropharmacological actions for virodhamine and analogs, besides their interactions with cannabinoid receptors function[27, 55]. Treatment of Neuroscreen-1 (NS-1) cells (a sub-clone of rat endocrine PC12 cells) with virodhamine produced significant inhibition of MAO activity. This observation confirms the potential uptake of virodhamine by neuronal cells. Virodhamine treatment has shown significant neuropharmacological action in peripheral systems as well as in brain *in vivo* in animal models [56-58]. These reports indicated the potential uptake of virodhamine by brain. Further studies would be required to determine the effect of virodhamine and related analogs on neuropharmacological functions associated with monoaminergic neurotransmission functions specially linked to effects mediated by MAO-B.

In conclusion, we have demonstrated that virodhamine is a time-dependent irreversible inhibitor of MAO-B. Further, we identified inhibitory effects of endocannabinoid virodhamine and related analogs on MAO-A and -B activity and studied enzyme-inhibition kinetics for virodhamine on MAO-B. Finally, we demonstrate the interaction profile and binding mode of virodhamine to MAO-B using Induced-Fit docking study. The selective inhibition of MAO-B of virodhamine shows the potential therapeutic application of this endocannabinoid for the treatment of Parkinson’s disease and Alzheimer’s disease.

Acknowledgements

This work was supported in part by grant P20GM104932 from the National Institute of General Medical Sciences. The content is solely the responsibility of the authors and does not necessarily represent the official views of the National Institutes of Health. This investigation was conducted in part in a facility constructed with support from research facilities improvement program C06RR14503 from the NIH. Thanks to the Mississippi Center for Supercomputing Research for computational time including with support of NSF 1338056. The authors also thank Janet A. Lambert (Associate R&D Biologist, The University of Mississippi, USA) for manuscript proofreading.

References

[1]. Youdim MB, Bakhle YS, Monoamine oxidase: isoforms and inhibitors in Parkinson's disease and depressive illness, Br J Pharmacol 147 Suppl 1 (2006) S287–96. [PubMed: 16402116]

[2]. Ramsay RR, Albreht A, Kinetics, mechanism, and inhibition of monoamine oxidase, Journal of Neural Transmission (2018) 1–25. [PubMed: 29260324]

[3]. Bach AW, Lan NC, Johnson DL, Abell CW, Bembenek ME, Kwan SW, Seeburg PH, Shih JC, cDNA cloning of human liver monoamine oxidase A and B: molecular basis of differences in enzymatic properties, Proc Natl Acad Sci U S A 85(13) (1988) 4934–8. [PubMed: 3387449]

[4]. Youdim MB, Edmondson D, Tipton KF, The therapeutic potential of monoamine oxidase inhibitors, Nat Rev Neurosci 7(4) (2006) 295–309. [PubMed: 16552415]

[5]. Tripathi AC, Upadhyay S, Paliwal S, Saraf SK, Privileged scaffolds as MAO inhibitors: Retrospect and prospects, European Journal of Medicinal Chemistry 145 (2018) 445–497. [PubMed: 29335210]

[6]. Stahl SM, Felker A, Monoamine oxidase inhibitors: a modern guide to an unrequited class of antidepressants, CNS Spectr 13(10) (2008) 855–70. [PubMed: 18955941]

[7]. Carradori S, Secci D, Petzer JP, MAO inhibitors and their wider applications: a patent review, Expert Opinion on Therapeutic Patents 28(3) (2018) 211–226. [PubMed: 29324067]

[8]. Horstink M, Tolosa E, Bonuccelli U, Deuschl G, Friedman A, Kanovsky P, Larsen JP, Lees A, Oertel W, Poewe W, Rascol O, Sampaio C, S. European Federation of Neurological, S. Movement Disorder Society-European, Review of the therapeutic management of Parkinson's disease. Report of a joint task force of the European Federation of Neurological Societies and the Movement Disorder Society-European Section. Part I: early (uncomplicated) Parkinson's disease, Eur J Neurol 13(11) (2006) 1170–85. [PubMed: 17038031]

[9]. Teixeira FG, Gago MF, Marques P, Moreira PS, Magalhães R, Sousa N, Salgado AJ, Safinamide: a new hope for Parkinson's disease?, Drug Discovery Today 23(3) (2018) 736–744. [PubMed: 29339106]

[10]. Riederer P, Danielczyk W, Grunblatt E, Monoamine oxidase-B inhibition in Alzheimer's disease, Neurotoxicology 25(1-2) (2004) 271–7. [PubMed: 14697902]

[11]. Piomelli D, The endocannabinoid system: a drug discovery perspective, Curr Opin Investig Drugs 6(7) (2005) 672–9.

[12]. Pacher P, Batkai S, Kunos G, The endocannabinoid system as an emerging target of pharmacotherapy, Pharmacol Rev 58(3) (2006) 389–462. [PubMed: 16968947]

[13]. Pertwee RG, Howlett AC, Abood ME, Alexander SPH, Di Marzo V, Elphick MR, Greasley PJ, Hansen HS, Kunos G, Mackie K, Mechoulam R, Ross RA, International Union of Basic and Clinical Pharmacology. LXXIX. Cannabinoid receptors and their ligands: Beyond CB1 and CB2, Pharmacological Reviews 62(4) (2010) 588–631. [PubMed: 21079038]

[14]. Fezza F, Bari M, Florio R, Talamonti E, Feole M, Maccarrone M, Endocannabinoids, related compounds and their metabolic routes, Molecules 19(11) (2014) 17078–106. [PubMed: 25347455]

[15]. Moranta D, Esteban S, Garcia-Sevilla JA, Differential effects of acute cannabinoid drug treatment, mediated by CB1 receptors, on the in vivo activity of tyrosine and tryptophan hydroxylase in the rat brain, Naunyn Schmiedebergs Arch Pharmacol 369(5) (2004) 516–24. [PubMed: 15064921]

[16]. Fisar Z, Inhibition of monoamine oxidase activity by cannabinoids, Naunyn Schmiedebergs Arch Pharmacol 381(6) (2010) 563–72. [PubMed: 20401651]

[17]. Rubino T, Sala M, Vigano D, Braida D, Castiglioni C, Limonta V, Guidali C, Realini N, Parolaro D, Cellular mechanisms underlying the anxiolytic effect of low doses of peripheral Delta9-tetrahydrocannabinol in rats, Neuropsychopharmacology 32(9) (2007) 2036–45. [PubMed: 17287821]

[18]. Szabo B, Schlicker E, Effects of cannabinoids on neurotransmission, Handb Exp Pharmacol (168) (2005) 327–65. [PubMed: 16596780]

[19]. Engler B, Freiman I, Urbanski M, Szabo B, Effects of exogenous and endogenous cannabinoids on GABAergic neurotransmission between the caudate-putamen and the globus pallidus in the mouse, J Pharmacol Exp Ther 316(2) (2006) 608–17. [PubMed: 16214880]

[20]. Bambico FR, Duranti A, Tontini A, Tarzia G, Gobbi G, Endocannabinoids in the treatment of mood disorders: evidence from animal models, Curr Pharm Des 15(14) (2009) 1623–46. [PubMed: 19442178]

[21]. Athanasiou A, Clarke AB, Turner AE, Kumaran NM, Vakilpour S, Smith PA, Bagiokou D, Bradshaw TD, Westwell AD, Fang L, Lobo DN, Constantinescu CS, Calabrese V, Loesch A, Alexander SP, Clothier RH, Kendall DA, Bates TE, Cannabinoid receptor agonists are mitochondrial inhibitors: a unified hypothesis of how cannabinoids modulate mitochondrial function and induce cell death, Biochem Biophys Res Commun 364(1) (2007) 131–7. [PubMed: 17931597]

[22]. Hill MN, Ho WS, Hillard CJ, Gorzalka BB, Differential effects of the antidepressants tranylcypromine and fluoxetine on limbic cannabinoid receptor binding and endocannabinoid contents, J Neural Transm (Vienna) 115(12) (2008) 1673–9. [PubMed: 18974922]

[23]. Hill MN, Carrier EJ, Ho WS, Shi L, Patel S, Gorzalka BB, Hillard CJ, Prolonged glucocorticoid treatment decreases cannabinoid CB1 receptor density in the hippocampus, Hippocampus 18(2) (2008) 221–6. [PubMed: 18058925]

[24]. Mazor M, Dvilansky A, Aharon M, Lazarovitz Z, Nathan I, Effect of cannabinoids on the activity of monoamine oxidase in normal human platelets, Arch Int Physiol Biochim 90(1) (1982) 15–20. [PubMed: 6179486]

[25]. Gawienowski AM, Chatterjee D, Anderson PJ, Epstein DL, Grant WM, Effect of delta 9-tetrahydrocannabinol on monoamine oxidase activity in bovine eye tissues, in vitro, Invest Ophthalmol Vis Sci 22(4) (1982) 482–5. [PubMed: 6277821]

[26]. Clarke DE, Jandhyala B, Acute and chronic effects of tetrahydrocannabinols on monoamide oxidase activity: possible vehicle/tetrahydrocannabinol interactions, Res Commun Chem Pathol Pharmacol 17(3) (1977) 471–80. [PubMed: 897340]

[27]. Porter AC, Sauer JM, Knierman MD, Becker GW, Berna MJ, Bao J, Nomikos GG, Carter P, Bymaster FP, Leese AB, Felder CC, Characterization of a novel endocannabinoid, virodhamine, with antagonist activity at the CB1 receptor, J Pharmacol Exp Ther 301(3) (2002) 1020–4. [PubMed: 12023533]

[28]. Ho WS, Hiley CR, Vasorelaxant activities of the putative endocannabinoid virodhamine in rat isolated small mesenteric artery, J Pharm Pharmacol 56(7) (2004) 869–75. [PubMed: 15233865]

[29]. Finberg JP, Update on the pharmacology of selective inhibitors of MAO-A and MAO-B: focus on modulation of CNS monoamine neurotransmitter release, Pharmacol Ther 143(2) (2014) 133–52. [PubMed: 24607445]

[30]. Chaurasiya ND, Gogineni V, Elokely KM, Leon F, Nunez MJ, Klein ML, Walker LA, Cutler SJ, Tekwani BL, Isolation of Acacetin from Calea urticifolia with Inhibitory Properties against Human Monoamine Oxidase-A and -B, J Nat Prod 79(10) (2016) 2538–2544. [PubMed: 27754693]

[31]. Parikh S, Sara H, Peter G, Charles C, Christopher P, A fluorescent-based, high-throughput assay for detecting inhibitors of human Monoamine Oxidase A and B, BD Biosciences Discovery Labware (2012) S02T081R2.

[32]. Chaurasiya ND, Shukla S, Tekwani BL, A Combined In Vitro Assay for Evaluation of Neurotrophic Activity and Cytotoxicity, SLAS Discov 22(6) (2017) 667–675. [PubMed: 28314119]

[33]. Son SY, Ma J, Kondou Y, Yoshimura M, Yamashita E, Tsukihara T, Structure of human monoamine oxidase A at 2.2-A resolution: the control of opening the entry for substrates/inhibitors, Proc Natl Acad Sci U S A 105(15) (2008) 5739–44. [PubMed: 18391214]

[34]. Binda C, Li M, Hubalek F, Restelli N, Edmondson DE, Mattevi A, Insights into the mode of inhibition of human mitochondrial monoamine oxidase B from high-resolution crystal structures, Proc Natl Acad Sci U S A 100(17) (2003) 9750–5. [PubMed: 12913124]

[35]. Schrödinger Release 2016-2: Maestro, LLC, New York, NY 2016.

[36]. Bonivento D, Milczek EM, McDonald GR, Binda C, Holt A, Edmondson DE, Mattevi A, Potentiation of ligand binding through cooperative effects in monoamine oxidase B, J Biol Chem 285(47) (2010) 36849–56. [PubMed: 20855894]

[37]. Binda C, Hubalek F, Li M, Herzig Y, Sterling J, Edmondson DE, Mattevi A, Crystal structures of monoamine oxidase B in complex with four inhibitors of the N-propargylaminoindan class, J Med Chem 47(7) (2004) 1767–74. [PubMed: 15027868]

[38]. Binda C, Aldeco M, Geldenhuys WJ, Tortorici M, Mattevi A, Edmondson DE, Molecular Insights into Human Monoamine Oxidase B Inhibition by the Glitazone Anti-Diabetes Drugs, ACS Med Chem Lett 3(1) (2011) 39–42. [PubMed: 22282722]

[39]. Binda C, Wang J, Pisani L, Caccia C, Carotti A, Salvati P, Edmondson DE, Mattevi A, Structures of human monoamine oxidase B complexes with selective noncovalent inhibitors: safinamide and coumarin analogs, J Med Chem 50(23) (2007) 5848–52. [PubMed: 17915852]

[40]. De Colibus L, Li M, Binda C, Lustig A, Edmondson DE, Mattevi A, Three-dimensional structure of human monoamine oxidase A (MAO A): relation to the structures of rat MAO A and human MAO B, Proc Natl Acad Sci U S A 102(36) (2005) 12684–9. [PubMed: 16129825]

[41]. Binda C, Wang J, Li M, Hubalek F, Mattevi A, Edmondson DE, Structural and mechanistic studies of arylalkylhydrazine inhibition of human monoamine oxidases A and B, Biochemistry 47(20) (2008) 5616–25. [PubMed: 18426226]

[42]. Schrödinger Release 2016-2: LigPrep, LLC, New York, NY, 2016.

[43]. Schrödinger Release 2016–2: Schrödinger Suite 2016-2 Induced Fit Docking protocol; Glide, LLC, New York, NY, 2016; Prime, Schrödinger, LLC, New York, NY, 2016.

[44]. Friesner RA, Murphy RB, Repasky MP, Frye LL, Greenwood JR, Halgren TA, Sanschagrin PC, Mainz DT, Extra precision glide: docking and scoring incorporating a model of hydrophobic enclosure for protein-ligand complexes, J Med Chem 49(21) (2006) 6177–96. [PubMed: 17034125]

[45]. Schrödinger Release 2016-2: Prime, LLC, New York, NY, 2016.

[46]. Glick J, Santoyo G, Casey PJ, Arachidonate and related unsaturated fatty acids selectively inactivate the guanine nucleotide-binding regulatory protein, Gz, J Biol Chem 271(6) (1996) 2949–54. [PubMed: 8621685]

[47]. Pearlman RJ, Aubrey KR, Vandenberg RJ, Arachidonic acid and anandamide have opposite modulatory actions at the glycine transporter, GLYT1a, J Neurochem 84(3) (2003) 592–601. [PubMed: 12558979]

[48]. Baur R, Gertsch J, Sigel E, Do N-arachidonyl-glycine (NA-glycine) and 2-arachidonoyl glycerol (2-AG) share mode of action and the binding site on the beta2 subunit of GABAA receptors?, PeerJ 1 (2013) e149. [PubMed: 24058880]

[49]. Finberg JP, Rabey JM, Inhibitors of MAO-A and MAO-B in Psychiatry and Neurology, Front Pharmacol 7 (2016) 340. [PubMed: 27803666]

[50]. Atiwannapat P, Arden PC, Stewart JW, Monoamine oxidase inhibitors for various psychiatric disorders and conditions, Psychiatric Annals 44(12) (2014) 567–573.

[51]. Janssen PAJ, Leysen JE, Megens AAHP, Awouters FHL, Does phenylethylamine act as an endogenous amphetamine in some patients?, International Journal of Neuropsychopharmacology 2(3) (1999) 229–240. [PubMed: 11281991]

[52]. Finberg JP, Lamensdorf I, Armoni T, Modification of dopamine release by selective inhibitors of MAO-B, Neurobiology (Bp) 8(2) (2000) 137–42. [PubMed: 11061211]

[53]. Dasgupta S, Mukherjee S, Mukhopadhyay BP, Banerjee A, Mishra DK, Recognition dynamics of dopamine to human Monoamine oxidase B: role of Leu171/Gln206 and conserved water molecules in the active site cavity, J Biomol Struct Dyn (2017) 1–24.

[54]. Laviolette SR, Grace AA, The roles of cannabinoid and dopamine receptor systems in neural emotional learning circuits: implications for schizophrenia and addiction, Cell Mol Life Sci 63(14) (2006) 1597–613. [PubMed: 16699809]

[55]. Di Marzo V, Bifulco M, De Petrocellis L, The endocannabinoid system and its therapeutic exploitation, Nat Rev Drug Discov 3(9) (2004) 771–84. [PubMed: 15340387]

[56]. Brusberg M, Arvidsson S, Kang D, Larsson H, Lindstrom E, Martinez V, CB1 receptors mediate the analgesic effects of cannabinoids on colorectal distension-induced visceral pain in rodents, J Neurosci 29(5) (2009) 1554–64. [PubMed: 19193902]

[57]. Richardson D, Ortori CA, Chapman V, Kendall DA, Barrett DA, Quantitative profiling of endocannabinoids and related compounds in rat brain using liquid chromatography-tandem electrospray ionization mass spectrometry, Anal Biochem 360(2) (2007) 216–26. [PubMed: 17141174]

[58]. Sun Y, Alexander SP, Garle MJ, Gibson CL, Hewitt K, Murphy SP, Kendall DA, Bennett AJ, Cannabinoid activation of PPAR alpha; a novel neuroprotective mechanism, Br J Pharmacol 152(5) (2007) 734–43. [PubMed: 17906680]

Chemical compounds studied in this article:

Anandamide (PubChem CID: 5281969); 2-Arachidonoylglycerol (PubChem CID: 5282280); Clorgyline (PubChem CID: 28767); Dimethyl sulfoxide (PubChem CID: 679); R-(−)-Deprenyl hydrochloride (PubChem CID: 5195); 4-Hydroxyquinoline (PubChem CID:69141); Kynuramine dihydrobromide (PubChem CID: 16219543); R-(+)-Methanandamide (PubChem CID: 6321351); Noladin ether (PubChem CID: 6483057); Oleylethanolamide (PubChem CID: 5283454); Phenelzine sulfate (PubChem CID: 61100); Potassium phosphate (PubChem CID: 516951); Safinamide (PubChem CID: 131682); Virodhamine trifluoroacetate (PubChem CID: 91691131).

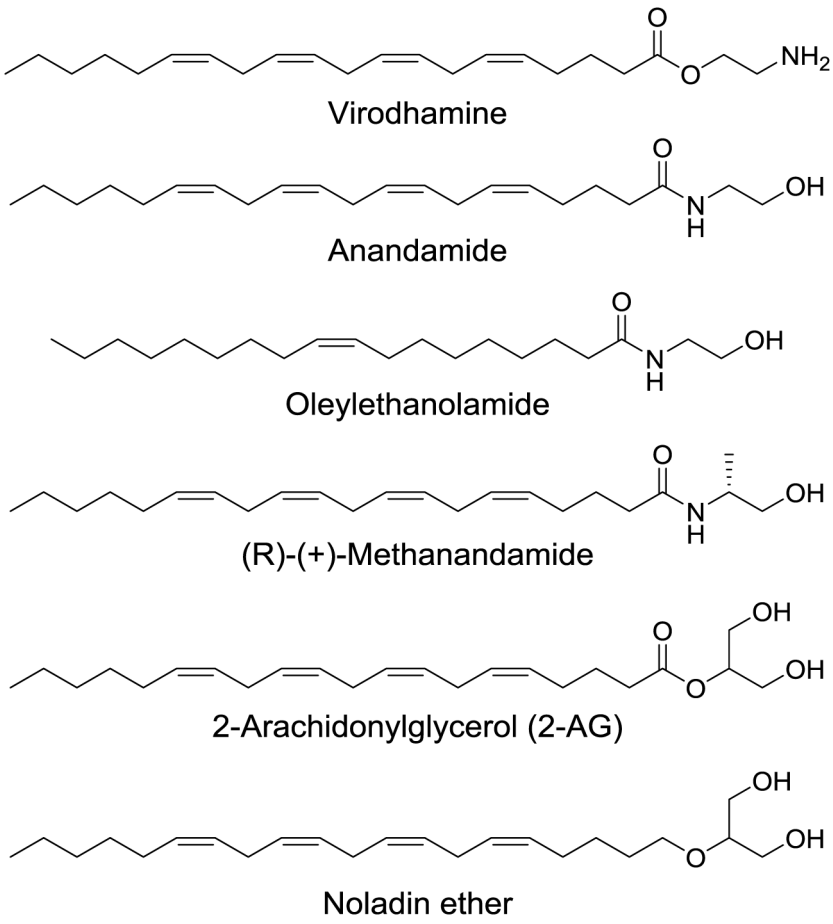

Fig. 1.

The **2D** structures of virodhamine and related analogs tested for inhibition of human MAO-A and -B.

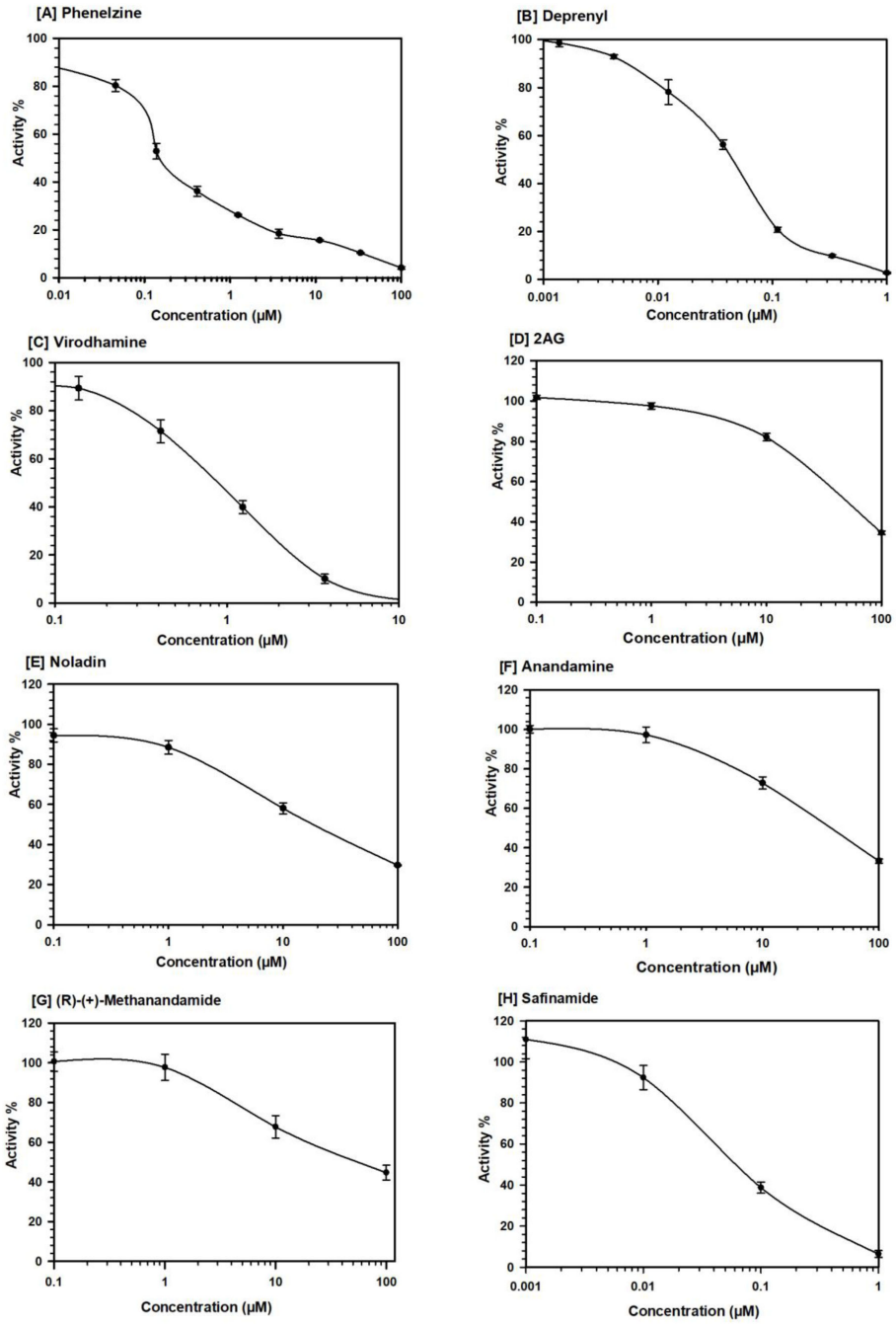

Fig. 2.

Concentration-response inhibition profile of human recombinant MAO-B by virodhamine and related analog. Phenelzine (a nonselective MAO inhibitor), deprenyl (a selective MAO-B inhibitor) and safinamide (a selective MAO-B reversible inhibitor) were tested simultaneously as reference standards. Each point represents the mean ± SD values of at least three observations.

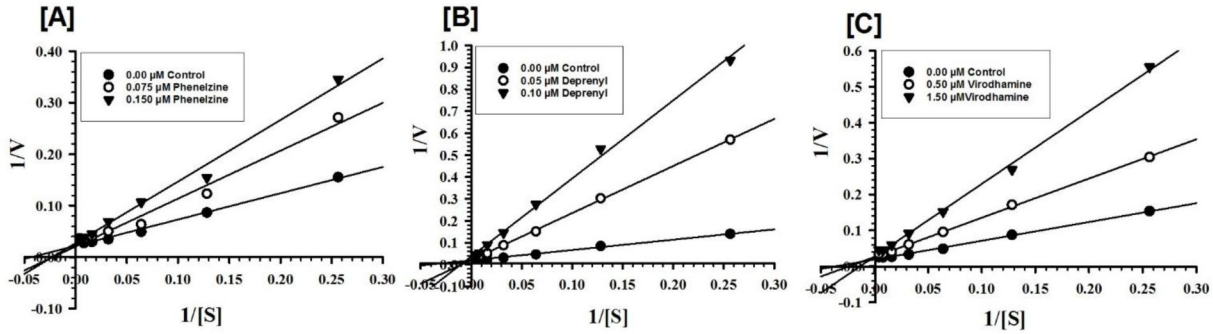

Fig. 3.

Kinetic characteristics of inhibition of recombinant human MAO-B with virodhamine [C]. Phenelzine [A] (a nonselective MAO inhibitor) and deprenyl [B] (a selective MAO-B inhibitor) were tested simultaneously as reference standards. Each point represents the mean ± S.D. of triplicate observations.

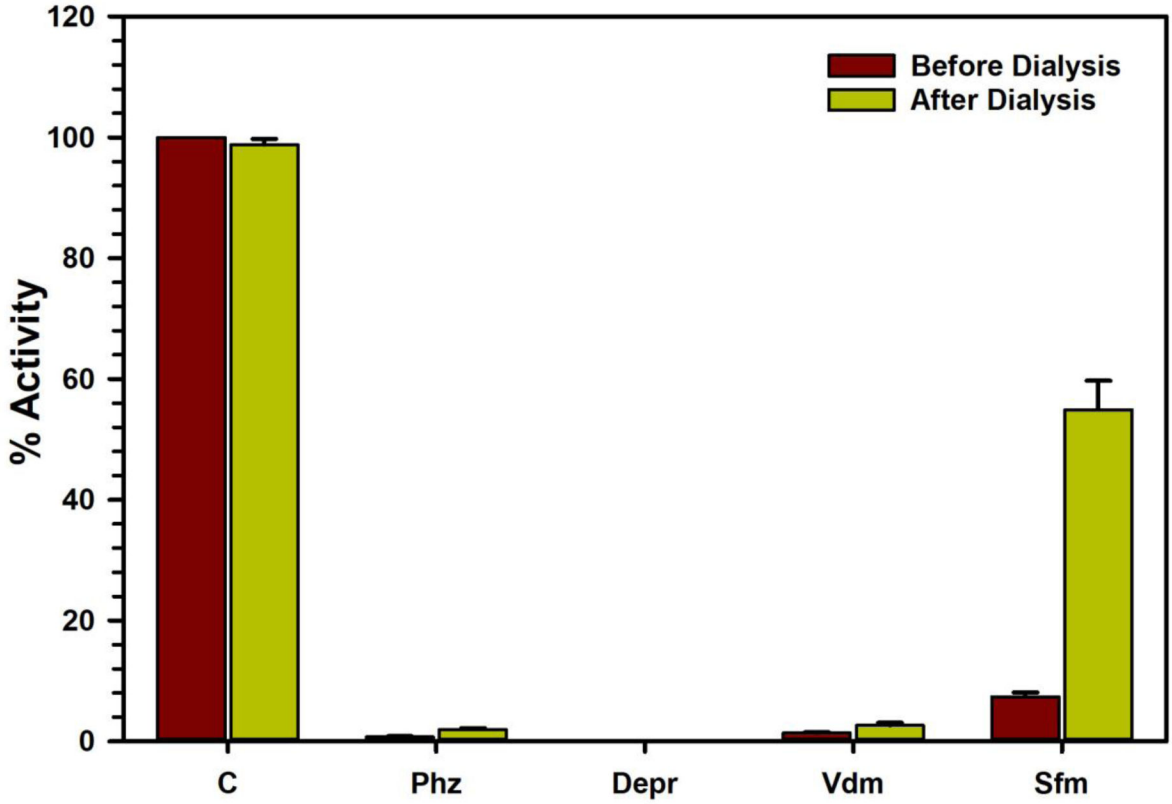

Fig. 4.

Analysis of the nature of virodhamine (Vdm) binding to human recombinant MAO-B by recovery of catalytic activity of the enzyme after dialysis dissociation, compared to the control reaction with no inhibitor present (C). Phenelzine (Phz) (a nonselective MAO inhibitor), deprenyl (Depr) (a selective MAO-B inhibitor) (both irreversible inhibitors) and safinamide (Sfm) (a selective MAO-B reversible inhibitor) were tested simultaneously as reference standards. Each bar shows mean ± S.D. for the triplicate values which were measured.

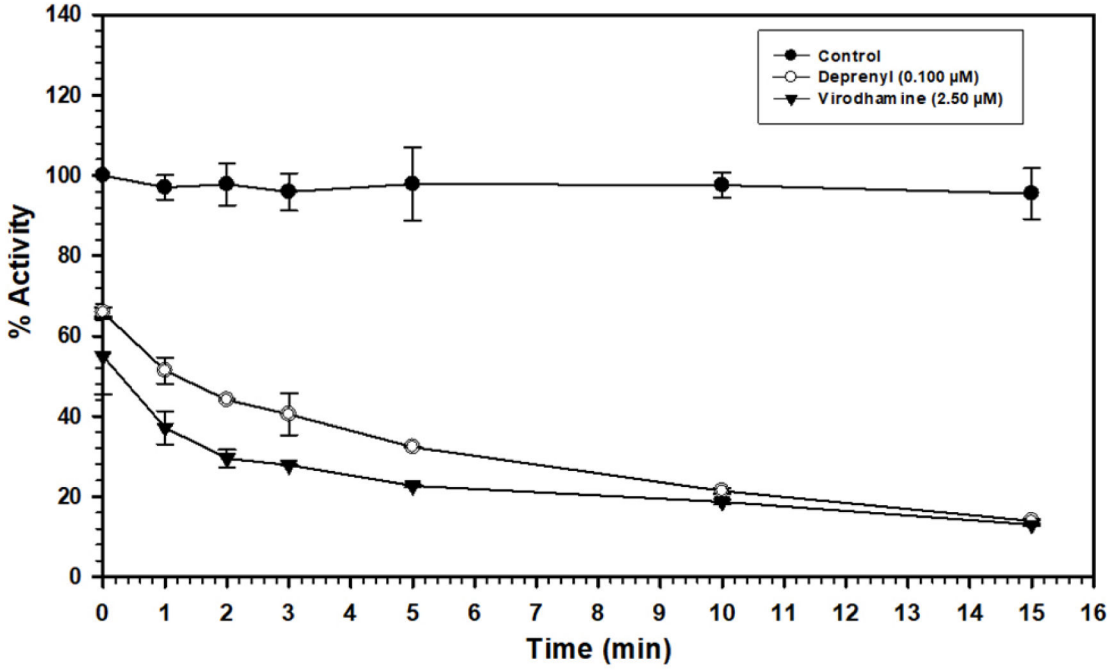

Fig. 5.

Time-dependent inhibition of recombinant human MAO-B by deprenyl (a selective MAO-B irreversible inhibitor) (0.100 µM) and virodhamine (2.50 µM), relative to the control with no inhibitor present. The remaining activity was expressed as % of activity. Each point represents mean ± SD of triplicate values.

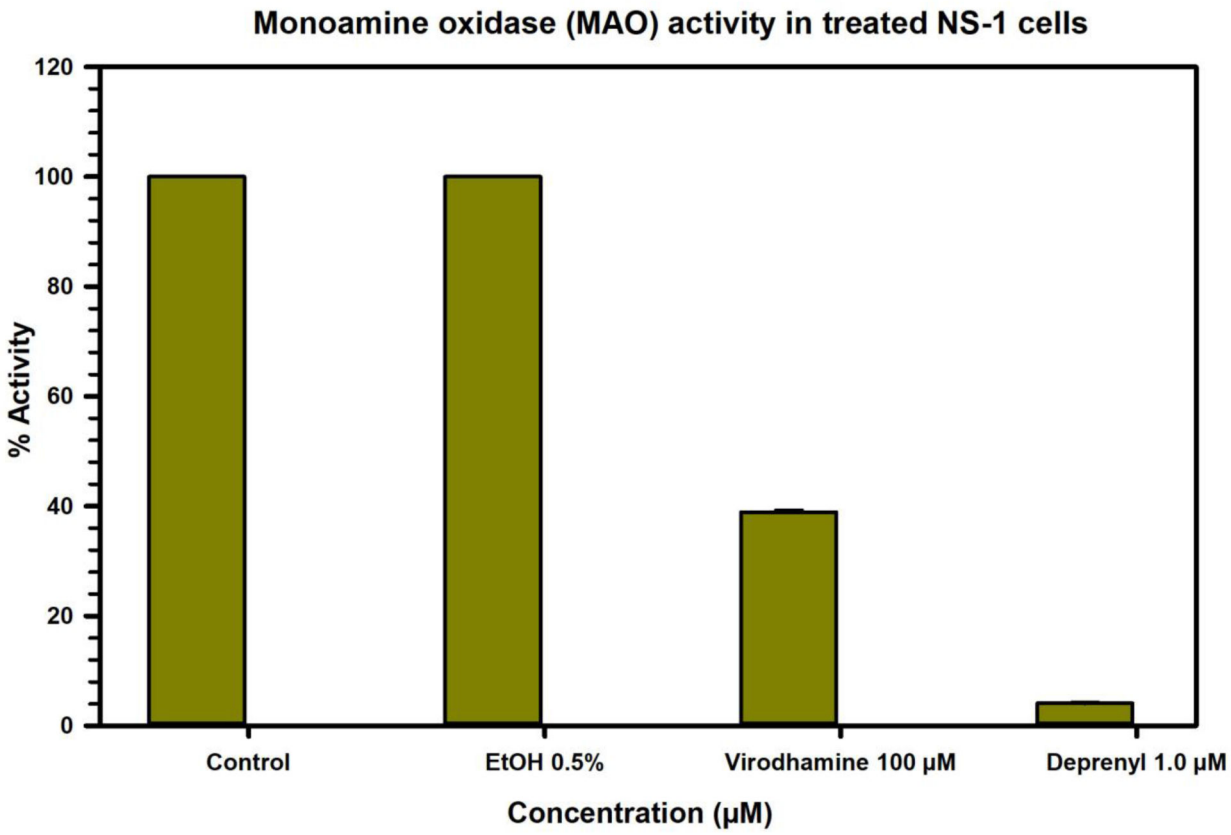

Fig 6.

Effect on MAO activity of treatment of Neuroscreen-1 (NS-1) cells with virodhamine, compared to ethanol, deprenyl. Each bar shows the mean values ± SD of three observations.

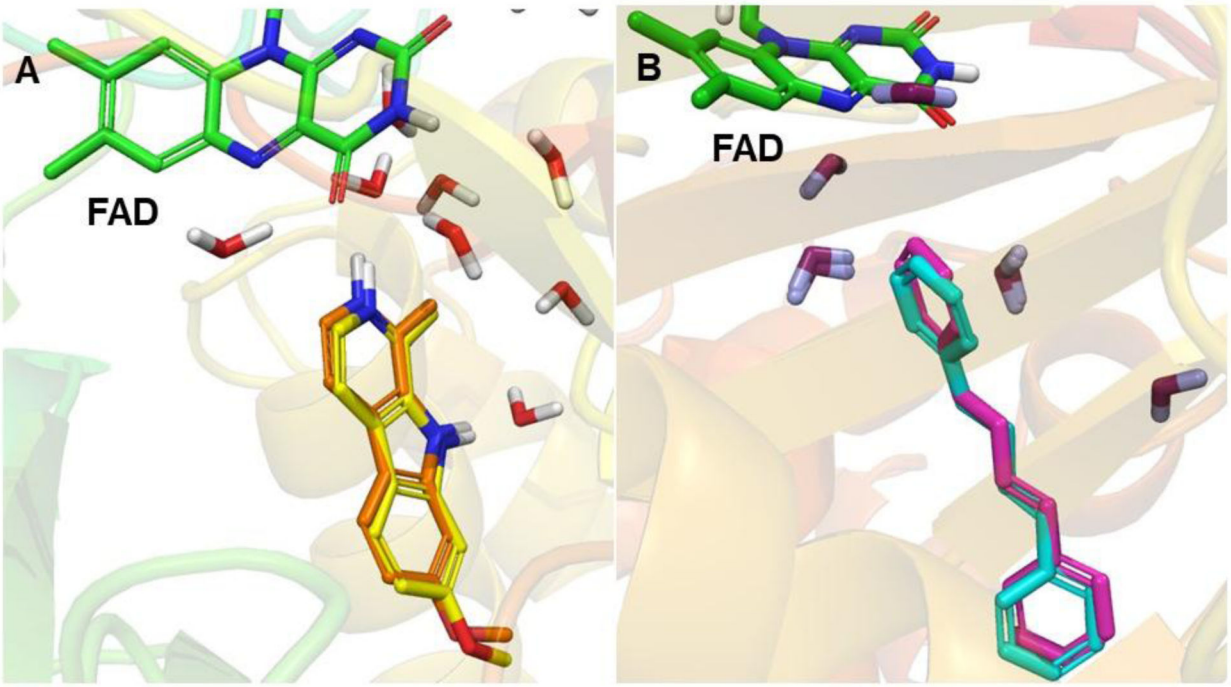

Fig. 7.

An overlay of the docked pose of (A) harmine (carbon in yellow) and co-crystallized harmine (carbon in orange) with the X-ray structure of MAO-A and (B) 1,4-diphenyl-2-butene (carbon in magenta) and co-crystallized 1,4-diphenyl-2-butene (carbon in cyan) with the X-ray structure of MAO-B. FAD (carbon in green) and some crystallographic waters are also shown.

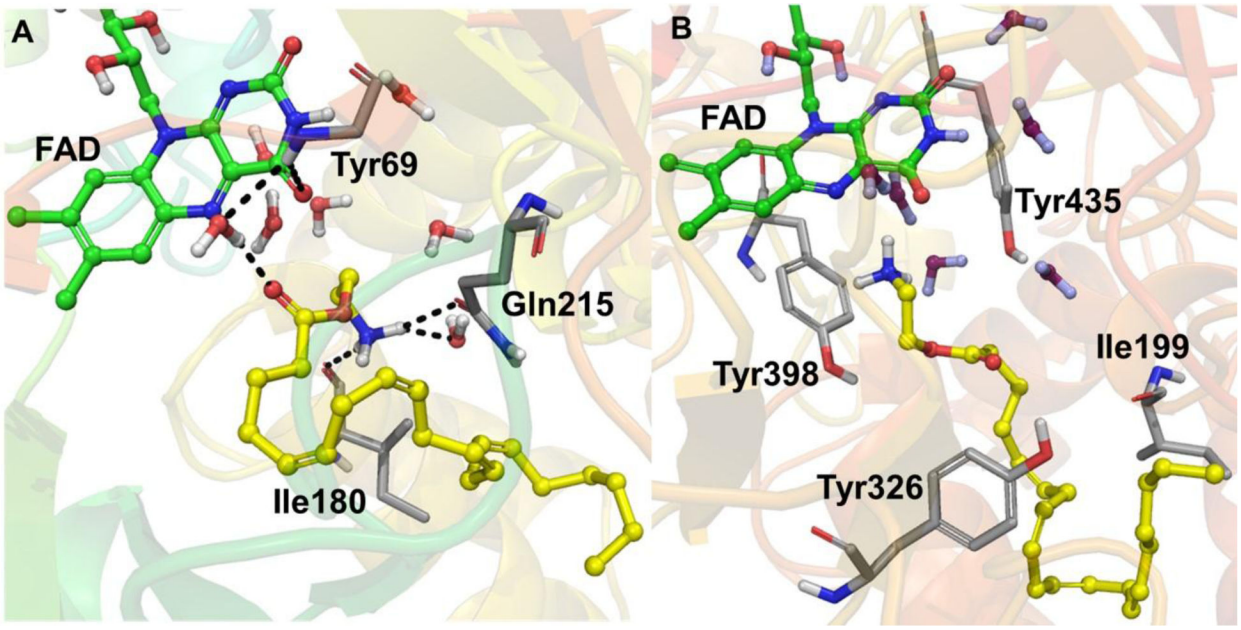

Fig. 8.

3D protein-ligand interactions of virodhamine (carbon in yellow, ball and stick model) with the X-ray crystal structures of (A) MAO-A and (B) MAO-B. The side chain of Tyr69 was hidden for clarity. FAD is represented with carbon in green, ball and stick model and some crystallographic waters are also shown. The important residues of MAO-A and -B are presented with carbon in grey. The black dashed lines represent H-bonding.

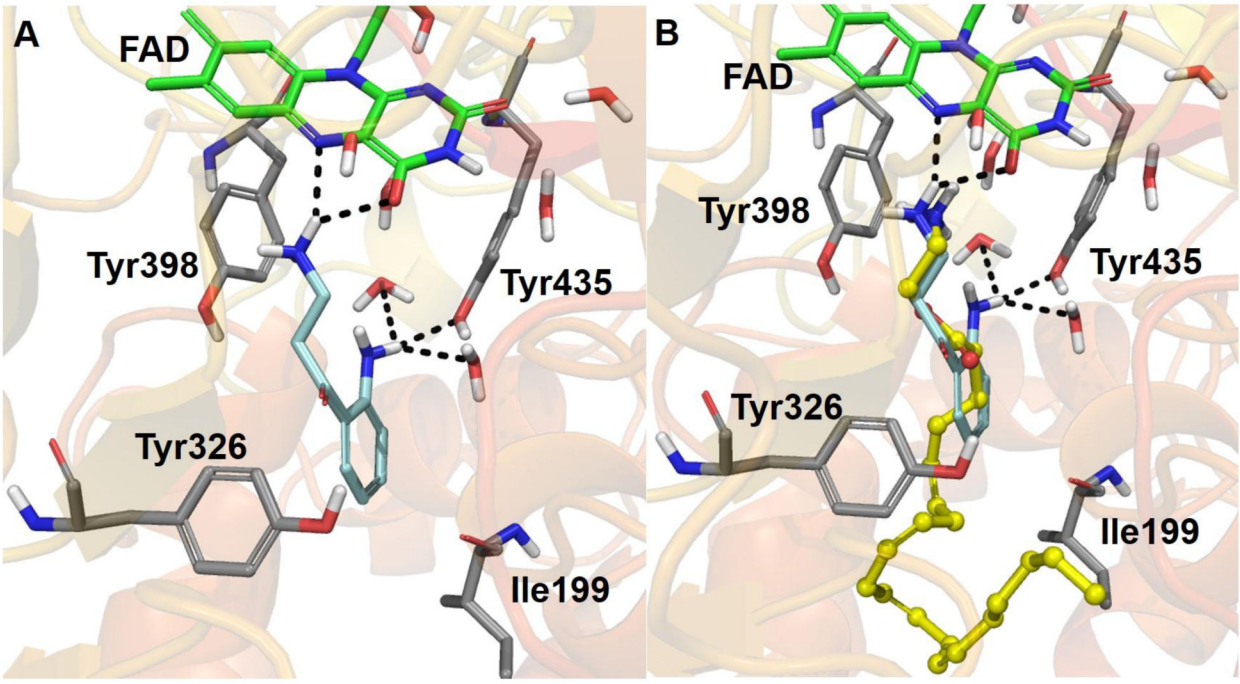

Fig. 9.

3D representation of protein-ligand interactions with MAO-B X-ray crystal structure for (A) kynuramine (carbon in cyan) and (B) overlay of kynuramine (carbon in cyan) and virodhamine (carbon in yellow, ball and stick model). FAD (carbon in green) and some crystallographic waters are also shown. The important residues of MAO-B are presented with carbon in grey. The black dashed lines represent H-bonding.

Table 1.

Inhibition (IC_{50} values) of recombinant human MAO-A and -B by virodhamine and related analogs.[a]

Compounds	MAO-A IC_{50} (μM) ± S.D.	MAO-B IC_{50} (μM) ± S.D.
2-AG	>100	50.53 ± 0.515
Noladin ether	>100	18.18 ± 1.45
(R)-(+)-Methanandamide	>100	51.090 ± 1.30
Oleylethanolamide	>100	>100
Anandamide	>100	39.98 ± 4.60
Virodhamine	38.70 ± 3.86	0.71 ± 0.04
Clorgyline (control)	0.004 ± 0.0005	ND
Deprenyl (control)	ND	0.049 ± 0.0036
Phenelzine (control)	0.213 ± 0.060	0.150 ± 0.015
Safinamide (control)	90.00 ± 2.470	0.060 ± 0.005

[a]The IC_{50} values computed from the concentration-response inhibition curves are mean ± S.D. of triplicate observations. ND = Not determined. Phenelzine (a nonselective MAO inhibitor), deprenyl (a selective MAO-B inhibitor), safinamide (a selective MAO-B inhibitor) and clorgyline (a selective MAO-A inhibitor) were tested simultaneously as reference standards.

Table 2.

Binding affinity constants (Ki) for inhibition of recombinant human MAO-B by virodhamine.[a]

Compounds	MAO-B	
	Ki (μM) ± S.D.	Type of Inhibition
Virodhamine	0.258±0.037	Mixed / Irreversible
Phenelzine	0.065±0.006	Mixed / Irreversible
Deprenyl	0.013±0.002	Mixed / Irreversible

[a]Values are mean ± S.D. of triplicate experiments. ND = Not determined. Phenelzine (a nonselective MAO inhibitor) and deprenyl (a selective MAO-B inhibitor) were tested simultaneously as reference standards.

Table 3.

Docking scores and binding free-energies of virodhamine and kynuramine with MAO-A and -B X-ray crystal structures.

Compounds	GlideScore (kcal/mol)		Binding free-energy (MM-GBSA) (kcal/mol)	
	MAO-A	MAO-B	MAO-A	MAO-B
Virodhamine	−10.17	−11.26	−33.97	−48.00
Kynuramine	Not determined	−7.67	Not determined	−36.71